The mechanism of the solid-state reaction between carbon nanotubes and nanocrystalline silicon under high pressure and at high temperature

2006 J. Phys.: Condens. Matter 18 2995

(http://iopscience.iop.org/0953-8984/18/11/006)

INSTITUTE OF PHYSICS PUBLISHING JOURNAL OF PHYSICS: CONDENSED MATTER

J. Phys.: Condens. Matter **18** (2006) 2995–3003 doi:10.1088/0953-8984/18/11/006

The mechanism of the solid-state reaction between carbon nanotubes and nanocrystalline silicon under high pressure and at high temperature

Yuejian Wang and T W Zerda

Department of Physics and Astronomy, Texas Christian University, TCU 298840, Fort Worth, TX 76129, USA

Received 23 November 2005
Published 27 February 2006
Online at stacks.iop.org/JPhysCM/18/2995

Abstract

An x-ray powder diffraction method was used to study the reaction between carbon nanotubes (CNT) and silicon (Si) nanosize powder at 2 GPa and temperatures varying from 1273 to 1370 K with different sintering times. Samples were obtained using the piston–cylinder system. On the basis of the Avrami–Erofeev model, we found the activation energy of silicon carbide (SiC) formation from CNT and Si to be 96 ± 30 kJ mol^{-1}. Analysis of x-ray diffraction patterns provided information on the domain sizes and microstrain in SiC. Extending the sintering time increased the grain sizes and decreased the microstrain in SiC, and increasing the temperature resulted in larger crystallites.

1. Introduction

Due to the formation of sp, sp^2, and sp^3 hybridized bonds, carbon (C) exists in numerous phases such as graphite, CNT, and diamond [1]. These different hybridizations lead to the significantly different features of carbon phases, e.g., diamond is the hardest material, but graphite is very soft. All carbon phases can react with Si to form SiC which is an important material and plays a key role in many fields. Sustained efforts have been devoted to studying the reaction between elemental carbon and Si. Gorovenko *et al* [2] investigated the high temperature interactions in the silicon–graphite system. They found that the activation energy for the reaction between micrometre size Si and graphite particles was 230 ± 20 kJ mol^{-1} and the process was limited by diffusion of carbon in liquid silicon. Previously, our group studied the kinetics of SiC formation from diamond and Si under high temperature and high pressure conditions. We concluded that the reaction was controlled by the diffusion of carbon atoms through the newly formed SiC layer with activated energy ranging from 170 ± 40 kJ mol^{-1} for nanodiamond to 260 ± 40 kJ mol^{-1} for micrometre size diamond [3]. To the best of our knowledge no information on the reaction between CNT and Si is currently available.

The carbon nanotube is a particular form of carbon, and since it was observed in 1990s [4], it has attracted extensive attention around the world. Because of its unique properties, it has

Table 1. Sintering conditions for samples.

Temperature (K)	Pressure (GPa)	Sintering time (s)
1270	2	60, 180, 300, 540, 780
1320		60, 180, 300, 540, 780
1370		60, 180, 300, 540, 780, 1020

been used to reinforce ceramic composites [5–10], including CNT/SiC composites [5, 10]. Most of works in this field were focused on processing and characterization of composites, and no studies on the kinetics of the reaction between CNT and Si have been published.

CNT could be used to reinforce diamond–SiC composites. In those composites SiC is produced by a chemical reaction between diamond and silicon and this phase forms a matrix in which diamond crystals are embedded. The strength of the composite is determined by the strength of the SiC phase. Qian *et al* demonstrated that when the SiC phase contained nanosize crystals, diamond–SiC composites had enhanced hardness and fracture toughness [13]. It is the microstructure (domain size and microstrain) that governs the mechanical properties of materials [11–14]. An investigation of the grain size and microstrain of crystals may indirectly provide valuable information on hardness and fracture toughness, two of the most important parameters characterizing nanocomposites.

In this work, we study the solid-state reaction between carbon nanotubes and nanosilicon under high pressure and high temperature conditions. X-ray powder diffraction was used to measure the degree of reaction, and the activation energy of SiC formation from CNT was determined by fitting the reaction rates to the Avrami–Erofeev model. Analysis of the shape of x-ray diffraction lines provided information on the average domain size and microstrains in SiC. Finally, we discuss possibilities for using CNT to reinforce diamond/SiC composites.

2. Experimental details

2.1. Sample preparation

In our experiments, the starting materials were multiwall carbon nanotubes, of purity better than 95%, and nanosize silicon powders, of grain size less than 70 nm and purity higher than 99%. Both were purchased from Nanostructured & Amorphous Materials Inc. (Los Alamos, New Mexico). The outer diameter of each CNT was about 60–100 nm, and their lengths were several micrometres. CNT were in the form of loose intertwined tubes. CNT and Si nanopowders in 1:1 molar ratio were dispersed in absolute alcohol by high energy sonication using an ultrasonic processor (Sonic & Materials, Inc.) at 60 W. The dispersing time was approximately 30 min. Then the mixture solution was poured into a culture dish to evaporate the alcohol. In order to prevent CNT and Si particles from separating in the solution, the dish holding the solution was placed inside a running ultrasonic cleaner. When the mixture of CNT and Si nanopowders was dry it was uniform, as verified by TEM analysis.

The samples listed in table 1 were fabricated by a high pressure sintering technique. Sintering experiments were run in a cylinder–piston-type cell using a 250-ton hydraulic press. Si–CNT mixtures were packed inside a cylindrical graphite heater placed inside the high pressure cell. Pressure was measured directly by a pressure gauge with a precision of about

0.1 GPa and temperature by a thermocouple placed inside the specimen with accuracy better than 25 K. The experiments were run according to the following protocol. The pressure was raised to 2 GPa at room temperature. Next, temperature was increased to the desired value at a rate of 200 K s^{-1}, and the samples were kept at that temperature for various times. Finally, temperature was decreased to the room level and pressure was released.

2.2. Sample characterization

X-ray diffraction (XRD) was used to characterize the phase composition and structure of specimens. X-ray diffraction patterns were recorded by a Philips diffractometer with Cu Kα_1 radiation ($\lambda = 1.540\,56$ Å), operated at 35 kV and 30 mA. The measurement range of 2θ was from 20° to 110°, and the exposure time was 3 s at each step of 0.02°. A large silicon crystal with minimal line broadening, supplied by the diffractometer manufacturer, was used to remove the instrumental contribution from the measured x-ray line profiles. The procedure used for peak refinement was developed by Howard and Snyder [15].

2.3. Kinetics of the reaction

It is common practice to use a dimensionless parameter α called the degree of reaction to express the kinetics equation of reaction. In our study, the degree of reaction is defined as

$$\alpha = \frac{m_{\mathrm{Si}}^{\mathrm{reacted}}}{m_{\mathrm{Si}}^{\mathrm{initial}}} = \frac{m_{\mathrm{Si}}^{\mathrm{reacted}}}{m_{\mathrm{Si}}^{\mathrm{reacted}} + m_{\mathrm{Si}}^{\mathrm{remaining}}}. \tag{1}$$

Due to the mass relationship between Si and SiC, we rearranged the above equation as follows [16]:

$$\alpha = \frac{0.700\,45 \times m_{\mathrm{SiC}}^{\mathrm{as-grown}}}{0.700\,45 \times m_{\mathrm{SiC}}^{\mathrm{as-grown}} + m_{\mathrm{Si}}^{\mathrm{remaining}}}. \tag{2}$$

The time dependent sintering parameter $\alpha(t)$ for various specimens was calculated from the intensity ratio of the diffraction peaks due to Si and SiC. This parameter reveals the change of the mass fraction of the product.

There are several approaches for describing a solid-state reaction. The commonest model for the nucleation and growth process was developed by Avrami and Erofeev [17, 18]. Nucleation starts at nucleation sites that already exist randomly dispersed in the precursor phase. The density of germ nuclei diminishes because some of them become growth nuclei for grains of new phase and grains grow by ingesting other nuclei [17]. The Avrami–Erofeev equation is represented as

$$\alpha(t) = 1 - \exp[-(kt)^m] \tag{3}$$

where k is the reaction rate constant and m is a parameter that is related to the reaction mechanism.

2.4. Procedure of evaluation of the x-ray diffraction profiles

Profile analysis of x-ray diffraction patterns has been widely used for evaluation of grain sizes and microstrains. Balzar and co-workers [19–23] have developed a simple methodology and below we provide some basic information regarding this technique. This double Voigt evaluation approach approximates the physically broadened (size–strain line broadening) diffraction profiles as a convolution of Gauss and Cauchy functions. The size and distortion

integral breadths of Cauchy (β_{SC} and β_{DC}) and Gauss (β_{SG} and β_{DG}) components comply with the convolution principle, and the relations have been given:

$$\beta_C = \beta_{SC} + \beta_{DC}\frac{s^2}{s_0^2} \tag{4}$$

$$\beta_G^2 = \beta_{SG}^2 + \beta_{DG}^2\frac{s^2}{s_0^2}. \tag{5}$$

β_{SC}, β_{DC}, β_{SG}, and β_{DG} could be obtained from at least two reflections. Surface- and volume-weighted domain sizes are directly expressed by the equations

$$\langle D\rangle_s = \frac{1}{2\beta_{SC}} \tag{6}$$

$$\langle D\rangle_v = \frac{\exp(k^2)}{\beta_{SG}}\,\mathrm{erfc}(k) \tag{7}$$

where $k = \beta_{SC}/(\pi^{1/2}\beta_{SG})$ is the characteristic integral breadth ratio of a Voigt function and $\mathrm{erfc}(k)$ is the error function complement. In addition, this method allows characterization of microstrains in crystals. Microstrains can be evaluated from the average distance L perpendicular to the diffracting planes and parameters β_{DC} and β_{DG}:

$$\langle \varepsilon^2(L)\rangle = \frac{1}{s_0^2}\left(\frac{\beta_{DG}^2}{2\pi} + \frac{\beta_{DC}}{\pi^2}\frac{1}{L}\right). \tag{8}$$

3. Results

We selected three sintering temperatures, 1270, 1320, and 1370 K. Under 2 GPa, all three temperatures are below the melting point of silicon. During the reaction, both silicon and CNT were in the solid state. Attempts to study the reaction at a lower temperature, 1170 K, failed because in a reasonable time we were unable to collect sufficient SiC for further analysis. At 1470 K the process was very fast and it was impossible to adequately control parameters of the reaction. In both cases experimental errors prevented us from determining reaction rates. Normally, good quality diamond–SiC composites are manufactured at pressures above 5 GPa where diamond is the stable form of carbon. Recently, it has been suggested that good quality diamond–SiC composites could be produced at much lower pressures, even as low as 2 GPa [24].

X-ray diffraction patterns were recorded for all specimens; an example is shown in figure 1. Characteristic peaks of Si, SiC, and CNT can be clearly observed, indicating that the reaction was incomplete. Only one phase of SiC, the hexagonal one also called the β phase, was detected. For each run, the amount of SiC was determined from intensities of Si(111) and SiC(111) peaks by using the calibration curve obtained from x-ray patterns of known quantities of SiC and Si. Here we consider Si(111) and SiC(111) peaks only, because (111) reflections of Si and SiC give rise to stronger peaks than other reflections and larger intensity peaks provide more accurate determination of the quantities of Si and SiC. When other peaks were used to estimate the quantity of SiC similar results were obtained; however, the error margins were greater, and these results were not included in further analysis. This result confirms that the specimens did not undergo texture evolution in the temperature region investigated. The degree of the reaction $\alpha(t)$ for each independent run was calculated using equation (2). The plots of $\alpha(t)$ versus t are shown in figure 2. The solid, dashed, and dotted lines represent the best Avrami–Erofeev fittings of $\alpha(t)$ for three different temperatures. The fitting parameters m and k of the Avrami–Erofeev equation are listed in table 2.

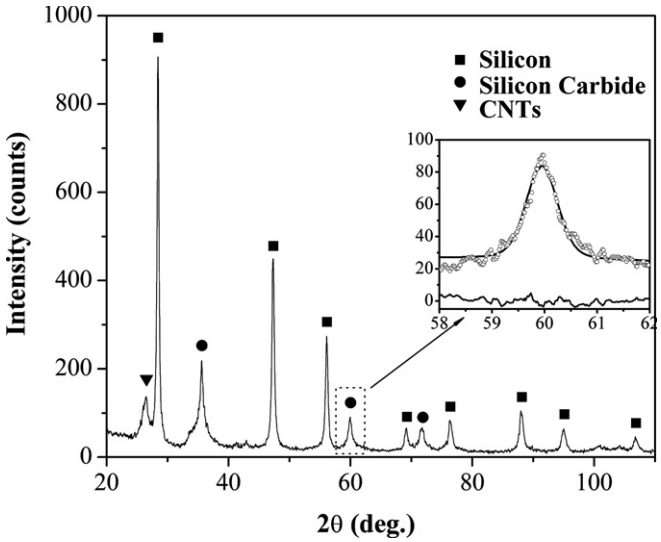

Figure 1. X-ray diffraction pattern of the sample obtained at 2 GPa, 1370 K, and sintered for 60 s. The inset represents measured (open circles) and fitted (solid line) diffraction profiles of SiC(220) obtained using the Voigt function, and the difference between the two sets of curves is shown in the bottom part of the inset.

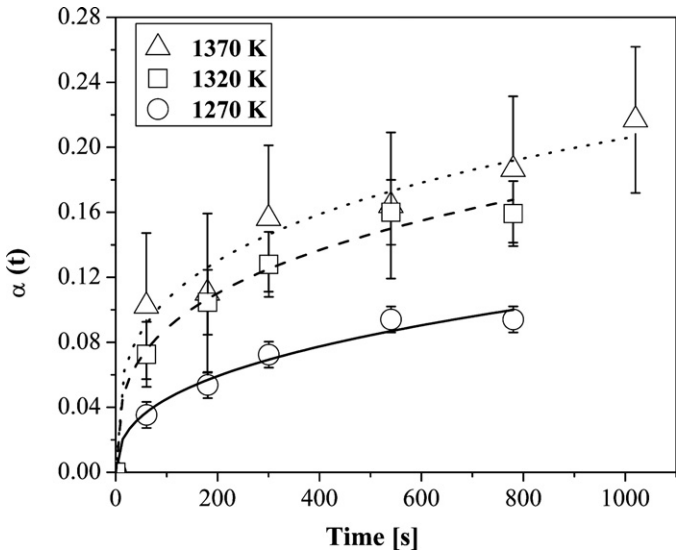

Figure 2. Plot of degree of reaction, α, versus time. Solid, dashed, and dotted lines represent the best fit of the Avrami–Erofeev equation to experimental data for the (111) reflections at 1270, 1320, and 1370 K, respectively.

According to Arrhenius law, the reaction rate constant is represented by the equation

$$k = A \cdot \exp\left(-\frac{E}{R \cdot T}\right) \tag{9}$$

where R is the gas constant and A is called the frequency factor. A plot of $\ln k$ as a function of the reciprocal temperature is shown in figure 3. The activation energy for the solid-state

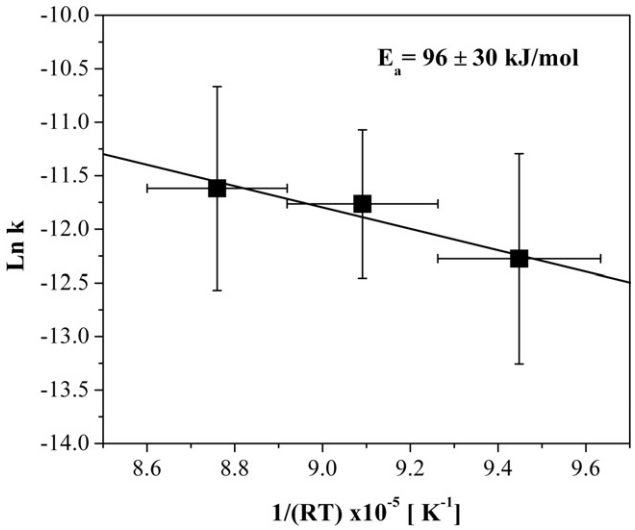

Figure 3. Arrhenius plot of the reaction rate constant k against the reciprocal temperature.

Table 2. Kinetics parameters of the Avrami–Erofeev model obtained by fitting experimental data to equation (3). Δk and Δm are estimated errors in determining parameters k and m.

T (K)	k (10^{-6}) (s^{-1})	Δk (10^{-6}) (s^{-1})	m (−)	Δm (−)
1270	4.7	3.5	0.4	0.05
1320	7.8	4.8	0.3	0.03
1370	9.0	6.7	0.3	0.04

reaction between Si and CNT under 2 GPa is 96 ± 30 kJ mol^{-1}, estimated from fitting the data to a straight line. This value is smaller than that for SiC manufactured from diamond [3] or graphite [2].

For domain sizes and microstrains of as-grown SiC, our analysis focused on (111) and (220) peaks of SiC. Other peaks were not taken into consideration due to their low intensities which may cause unexpected errors in calculations. Both peaks were refined by the double Voigt multiple-line integral breadth method, and one example of the refined (220) peak is shown in the inset of figure 1. Using (111) and (220) peaks as input profiles, the domain sizes and microstrains of as-grown SiC have been derived, and the results are shown in figure 4 and table 3.

At similar sintering times, the higher temperature resulted in larger domain size. At a constant temperature the average domain size initially increased, but with elapsed sintering time this growth process slowed down and eventually stopped. The microstrains inside the as-fabricated SiC are listed in table 3. It is seen that strain decreases with the sintering time. As expected, higher temperature leads to a smaller concentration of defects.

4. Discussion and summary

The activated energy of SiC formation from CNT and Si is lower than the reported values for reactions when carbon was in the form of diamond or graphite. We may trace this phenomenon back to the different atomic structures of the precursors. Diamond is the sp^3 hybridization

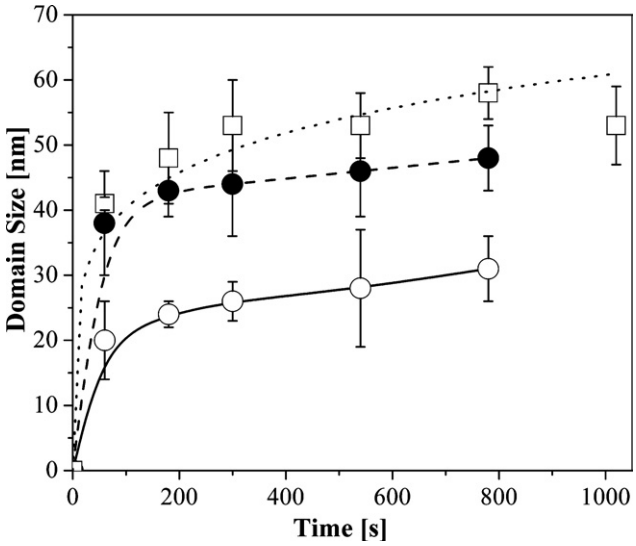

Figure 4. Plot of the domain size of as-grown SiC. ○, ● and □ represent the experimental data obtained at 1270, 1320, and 1370 K, respectively. Solid, dashed, and dotted lines represent the best fits of the experimental data obtained at the corresponding temperatures 1270, 1320, and 1370 K.

Table 3. Microstrains inside the as-fabricated SiC.

Sintering time (s)	ε (10^{-4}) at 1270 K	ε (10^{-4}) at 1320 K	ε (10^{-4}) at 1370 K
60	62 ± 16	58 ± 16	38 ± 4
180	51 ± 17	32 ± 13	37 ± 4
300	49 ± 20	48 ± 16	35 ± 3
540	45 ± 12	25 ± 12	35 ± 3
780	47 ± 16	48 ± 18	22 ± 3
1020			29 ± 2

of carbon, and a three-dimensional (3D) network is formed by binding the tetrahedral unit structures together. The bond between two atoms in diamond crystal is very strong. In graphite the sp^2 hybridization results in strong C–C bonds within graphene layers. A perfect CNT is a graphene sheet seamlessly wrapped into a cylindrical tube. Experimental results however clearly indicate that CNT possess many defects; for example, Mawhinney *et al* [25] reported that several per cent of carbon atoms on the CNT walls can be located at defective sites. The most common defects are the so-called Stone–Wales (SW) defects, which are pairs of adjacent five-and seven-member rings. The SW defects are formed unavoidably during nanotube synthesis process, since additional pairing of a heptagon with a pentagon is energetically favourable and a high concentration of these defects may lead to tube bending and changed diameter. We have observed this behaviour in TEM images of carbon nanotubes recorded prior to the reaction. It is generally accepted that SW defect sites trigger chemical reactions between CNT and other materials [26, 27]. In our case, under high temperature and high pressure conditions CNT are compressed and thus the number of defects in probably increased. In addition, under these conditions, SW defects can glide, twist, and distort; thereby some C–C bonds may brake. It is then energetically favourable for these dangling bonds to react with Si

atoms. Of course, other defects, such as vacancies, impurities, and kinks, may also be present and their combined effect could further lower the activation energy.

We assume that the reaction with silicon starts at SW defects on outer walls of multiwall CNT. Then SiC grows along the tube outer walls but also radially. A high density of defects results in numerous nucleation sites. As the grains grow they overlap and coalesce. The average size of SiC domains varies between 20 and 50 nm. Of course, continuing the reaction for an extended period of time at increasingly higher temperature facilitates growth of the crystallites. As expected, analysis of x-ray diffractograms indicated that an additional benefit of conducting the reaction at high temperature is an annealed structure with a dramatically reduced population of strains.

Zhao *et al* [13] showed experimental evidence that reduction of the average size of SiC crystallites from tens of microns down to about 20 nm increased the fracture toughness of diamond/SiC composites. They claimed that the nanosize SiC matrix would decrease the ability of cracks to propagate, and this mobility reduction thus leads to an improvement of the fracture toughness of the composites. They also showed that a lower population of dislocations enhances the hardness of the SiC matrix in which diamond crystals are embedded. It is very difficult to realize a nanostructured SiC phase in diamond composites, and Zhao *et al* had to apply special preparation techniques to achieve that goal.

The results of this study indicate that a nanostructured SiC matrix could be realized by a reaction between silicon and CNT. The nanosize crystallites and low strains of as-fabricated SiC could improve mechanical properties of composites. In the future, we plan to mix diamond crystals with a silicon/CNT mixture and then conduct high temperature sintering of diamond based composites at pressures higher than 5 GPa.

In summary, the solid-state reaction between CNT and Si has been investigated under high pressure and high temperature conditions. We focused attention on the kinetics study and microstructure analysis. Our results demonstrate that CNT may have higher chemical reactivity than other forms of elemental carbon, which could be ascribed to a high population of defects on the CNT surface. X-ray analysis shows that higher temperature created larger size SiC grains with low strains. Our results are of long-term application significance because they demonstrate that CNT could be used to design and manufacture CNT–SiC nanocomposites with a strong nanocrystalline bonding matrix and, conceivably, with both enhanced fracture toughness and high hardness which could be applied in harsh environments as well as in diamond composites.

Acknowledgment

This study was supported by the grant NSF-DMR 0502136.

References

[1] Miller E D, Nesting D C and Badding J V 1997 *Chem. Mater.* **9** 18
[2] Gorovenko V I, Knyazik V A and Shteinberg A S 1993 *Ceram. Int.* **19** 129
[3] Pantea C, Voronin G A, Zerda T W, Zhang J, Wang L, Wang Y, Uchida T and Zhao Y 2005 *Diamond. Relat. Mater.* **14** 1611–5
[4] Iijima S 1991 *Nature* **354** 56
[5] Ma R Z, Wu J, Wei B Q, Liang J and Wu D H 1998 *J. Mater. Sci.* **33** 5243
[6] An J-W, You D-H and Lim D-S 2003 *Wear* **255** 677
[7] Peigney A, Flahaut E, Laurent C, Chastel F and Rousset A 2002 *Chem. Phys. Lett.* **352** 20
[8] Balazsi C, Konya Z, Weber F, Biro L P and Arato P 2003 *Mater. Sci. Eng.* C **23** 1133
[9] Zhan G-D, Kuntz J D, Wan J and Mukherjee A K 2003 *Nat. Mater.* **2** 38
[10] Wang Y, Voronin G A, Zerda T W and Winarski A 2005 *J. Phys.: Condens. Matter* **18** 275–82

[11] Veprek S 2000 *Handbook of Ceramic Hard Materials* ed R Reidel (Weinheim: Wiley–VCH) pp 104–39
[12] Reimanis I E 1997 *Mater. Sci. Eng.* A **237** 159
[13] Zhao Y, Qian J, Daemen L, Pantea C, Zhang J and Zerda T W 2004 *Appl. Phys. Lett.* **84** 1356
[14] Qian J, Pantea C, Voronin G A and Zerda T W 2001 *J. Appl. Phys.* **90** 1632
[15] Howard S A and Snyder R L 1989 *J. Appl. Crystallogr.* **22** 238–43
[16] Pantea C 2004 Diamond–silicon reaction under high pressure–high temperature condition *Doctoral Thesis* Texas Christian University, Fort Worth, TX
[17] Avrami M 1939 *J. Chem. Phys.* **7** 1103
[18] Erofeev B V 1946 *C. R. Acad. Sci.* **52** 511
[19] Balzar D 1995 *J. Appl. Crystallogr.* **28** 244–5
[20] Balzar D and Ledbetter H 1997 *Adv. X-ray Anal.* **39** 457–64
[21] Balzar D 1992 *J. Appl. Crystallogr.* **25** 559–70
[22] Balzar D and Ledbetter H 1993 *J. Appl. Crystallogr.* **26** 97–103
[23] Balzar D 1999 *Defect and Microstructure Analysis from Diffraction (International Union of Crystallography Monographs on Crystallography No. 10)* ed R L Snyder, H J Bunge and J Fiala (New York: Oxford University Press) pp 94–126
[24] Ringwood A E 1988 *Australian Patent Specification* 601561
[25] Mawhinney D B, Naumenko V, Kuznetzova A, Yates J T, Liu J and Smalley R E 2000 *Chem. Phys. Lett.* **324** 213
[26] Chakrapani N, Zhang Y M, Nayak S K, Moore J A, Carroll D L, Choi Y Y and Ajayan P M 2003 *J. Phys. Chem.* B **107** 9308
[27] Picozzi S, Santucci S, Lozzi L, Valentini L and Delley B 2004 *J. Chem. Phys.* **120** 7147